Cancellation of photoinduced absorption in metal nanoparticle composites through a counterintuitive consequence of local field effects

David D. Smith

Space Sciences Laboratory, NASA Marshall Space Flight Center, ES-76, Huntsville, Alabama 35812

George Fischer

Rome Laboratory, Photonics Materials Branch, Hanscom Air Force Base, Massachusetts 01731

Robert W. Boyd

The Institute of Optics, University of Rochester, Rochester, New York 14627

Don A. Gregory

Department of Physics, University of Alabama in Huntsville, Huntsville, Alabama 35899

Received September 16, 1996; revised manuscript received March 10, 1997

By applying the Maxwell Garnett model to gold nanoparticles in water we deduce a value of Im $\chi_i^{(3)} = 1.1 \times 10^{-7}$ esu for the imaginary part of the cubic susceptibility for gold corresponding to a Fermi smearing mechanism. We also demonstrate a sign reversal in the nonlinear absorption for gold particles in 1, 1′, 3, 3, 3′, 3′-hexamethylindotricarbocyanine iodide. Although the imaginary part of $\chi^{(3)}$ is positive for each component by itself, remarkably the imaginary part of $\chi^{(3)}$ is negative for the colloid as a whole. We show that the nonlinearity of the host must be considered and that the sign reversal in $\chi^{(3)}$ is a result of the fact that at the surface plasmon resonance the local field factor has an imaginary component that arises from a phase shift between the applied field and the local field inside the particle. © 1997 Optical Society of America [S0740-3224(97)03807-1]

1. INTRODUCTION

Many devices have been proposed to take advantage of the intensity-dependent refractive index in various materials for all-optical switching. However, many materials with a large real part of the cubic nonlinearity have an associated high imaginary part that is due to resonant enhancement of a single-photon or multiphoton nature. Mizrahi *et al.* have shown that two-photon absorption (TPA) places a fundamental constraint on the usefulness of any high $\chi^{(3)}$ material.[1] Semiconductors, for example, are constrained to energies below half of the band gap to avoid TPA.[2] The current strategy for avoiding TPA is to search for a truly nonresonant operating wavelength. Here we present an alternative approach based on materials architecture for eliminating induced absorption. Specifically, this study demonstrates that the nonlinear absorption in a material can be canceled by the addition of small metal particles.

This approach is possible because of a counterintuitive consequence of local field effects that was first recognized by Hache *et al.*,[3] who found that for gold nanoparticles in glass the colloid as a whole demonstrated saturable absorption. However, the metal itself was thought to demonstrate induced absorption. Embedding the particles in a glassy matrix altered the sign of the nonlinear absorption as a result of the local field correction. The implication of the finding of Hache *et al.* is that there is a concentration somewhere between pure gold and the colloidal gold glass at which the imaginary part of the cubic susceptibility goes to zero. In fact, if the sign of Im $\chi^{(3)}$ is the same for each component, then by necessity there will actually be two concentrations at which Im $\chi^{(3)} = 0$. The smaller concentration crossing point is obviously more useful, because it entails a lower amount of linear absorption and to fabricate poses less of a challenge.

The linear optical properties of composite materials can be treated by the Maxwell Garnett model, which assumes small concentrations of spherical inclusions embedded in a continuous host medium.[4] Maxwell Garnett realized that the Lorentz local field could be used to find an effective dielectric constant for a medium consisting of a dispersion of conducting particles much smaller than the wavelength of light. Metal colloids display many different colors because of the surface plasmon resonance that occurs at the interface between the metal and the dielectric, and Maxwell Garnett hoped to use this effective dielectric constant to predict the colors that would be observed. The relation demonstrates that a medium

0740-3224/97/0701625-07$10.00

consisting of small distributed inclusion particles is optically equivalent to a medium with dielectric constant ϵ given by

$$\epsilon = \epsilon_h \frac{1 + 2\eta f}{1 - \eta f}, \tag{1}$$

where

$$\eta \equiv \frac{\epsilon_i - \epsilon_h}{\epsilon_i + 2\epsilon_h}. \tag{2}$$

The subscripts i and h denote inclusion and host values, respectively, and f represents the (metal) volume concentration or fill fraction. Note that as f approaches zero, ϵ approaches ϵ_h, as expected. Moreover, ϵ depends only on f and the dielectric constants of the constituents and not on the size or separation of the individual spheres. In other words, the Maxwell Garnett result does not take into account polydispersity or agglomeration.

The model has been extended to the case of nonlinear inclusions in a linear host by Ricard *et al.*[5] and more recently to the case of nonlinear inclusions in a nonlinear host by Sipe and Boyd.[6] For linearly polarized light, if both the host and inclusions are assumed to be nonlinear, the third-order susceptibility of a composite material is related to that of its constituents by the relation[6]

$$\chi^{(3)} = f q_i^2 |q_i|^2 \chi_i^{(3)} + q_h^2 |q_h|^2 [(1 - f) + xf] \chi_h^{(3)}, \tag{3}$$

where

$$x \equiv \frac{8}{5}\eta^2 |\eta|^2 + \frac{6}{5}\eta |\eta|^2 + \frac{2}{5}\eta^3 + \frac{18}{5}(|\eta|^2 + \eta^2). \tag{4}$$

The quantity q_i refers to the local field factor in the inclusions, whereas q_h is the local field factor in the host or the cavity field factor. The local field factors are[6]

$$q_i = \frac{\epsilon + 2\epsilon_h}{\epsilon_i + 2\epsilon_h}, \tag{5}$$

$$q_h = \frac{\epsilon + 2\epsilon_h}{3\epsilon_h}. \tag{6}$$

Although in general the local field factors are nonlinear functions of the field strength, this field dependence can be ignored here because we are interested only in the concentration dependence of $\chi^{(3)}$ and because the experiments to follow will be performed at a single value of the optical field.

Because of the asymmetry of the Maxwell Garnett model, rather than treating both materials as inclusions in a continuous effective medium, one component is treated as a continuous host medium. The nonuniform geometry of the host in the vicinity of the inclusions then prohibits the assumption that the nonlinear polarization is uniform across it, leaving some remaining volume bound charge. The field about each inclusion is dipolar so that dipole coupling interactions become more significant near each inclusion. The asymmetry in the Maxwell Garnett approach can clearly be seen in Eq. (3). The $(1 - f)$ terms in the host contribution take into account the nonlinear response of the host that is due only to the cavity field, whereas the f terms account for the small additional response of the host material near each inclusion.

The Maxwell Garnett model is not valid for large fill fractions precisely because of this asymmetry. A more universal theory (such as Bruggeman's effective medium theory,[7] which treats both components symmetrically) would take into account the dependence of the effective dielectric constant on the microscopic structural geometry of the composite, which becomes more important at larger fill fractions as percolation begins to occur. For the composite geometries discussed here, however, the metal volume fractions are small enough for the Maxwell Garnett model to apply.

Although Eq. (3) is useful for predicting $\chi^{(3)}$ over the full range of f (within the constraints mentioned above), it provides little intuitive insight because it is nonlinear in f. Now consider only a small range of fill fractions sufficient for predicting the lower-concentration $\mathrm{Im}\,\chi^{(3)} = 0$ position discussed above. For small fill fractions we have $\epsilon \approx \epsilon_h$ and $q_h \approx 1$ so that

$$\chi^{(3)} = f q_i^2 |q_i|^2 \chi_i^{(3)} + \chi_h^{(3)}. \tag{7}$$

Equation (7) is linear in f, with a slope determined by $q_i^2 |q_i|^2 \chi_i^{(3)}$ and an intercept determined by $\chi_h^{(3)}$. Remarkably, a cancellation of the two contributions can occur even though the sign of $\chi^{(3)}$ for each component is the same. This is because at the surface plasmon resonance we have the condition that

$$\epsilon_i'(\omega_s) = -2\epsilon_h', \tag{8}$$

where ω_s is the surface plasmon resonance frequency, primed quantities are real, and double-primed quantities are imaginary. The local field factor then becomes $q_i \approx 3\epsilon_h'/i\epsilon_i''$ for hosts without significant linear absorption. Hence, at the surface plasmon resonance, the local field factor becomes mainly imaginary (thus $q_i^2 < 0$) so that if $\chi_h^{(3)}$ and $\chi_i^{(3)}$ have the same sign there will be a sign reversal in $\chi^{(3)}$ at some fill fraction.

Let us examine the physical reason for this sign reversal in more detail. As already stated, the sign reversal in $\chi^{(3)}$ is a result of the fact that at the surface plasmon resonance the local field factor becomes mainly imaginary. What does it mean that the local field factor is imaginary, though? The local field factor q_i is the ratio of the field inside an inclusion $\mathbf{e}$ to the externally applied field $\mathbf{E}$. Both of these fields are vector quantities so that the local field factor describes the difference between the fields in phase as well as in magnitude. Hence a complex local field factor corresponds to a phase difference between the field inside an inclusion and the externally applied field. At the surface plasmon resonance the local field factor is mainly imaginary (for host materials without significant linear loss) and negative so that $\mathbf{e}$ is out of phase with $\mathbf{E}$, lagging behind by $-\pi/2$.

The general expression for the phase shift ϕ between $\mathbf{e}$ and $\mathbf{E}$ for small fill fractions is

$$\tan^{-1}\phi = \frac{\epsilon_i'\epsilon_h'' - \epsilon_i''\epsilon_h'}{\epsilon_i'\epsilon_h' + \epsilon_i''\epsilon_h'' + 2(\epsilon_h'^2 + \epsilon_h''^2)}, \tag{9}$$

as obtained from Eq. (5). At the surface plasmon frequency ω_s, the relation simplifies to

$$\tan^{-1}\phi = -(\epsilon_h'/\epsilon_h''). \tag{10}$$

Hence if the host is lossless (so that $\epsilon_h'' = 0$) then $\phi = -\pi/2$. As the linear absorption of the host increases, the phase shift decreases toward $\phi = -\pi$. For a lossless host at an arbitrary applied frequency the relation becomes

$$\tan^{-1}\phi = -\frac{\epsilon_i''}{\epsilon_i' + 2\epsilon_h'}. \tag{11}$$

At ω_s we again obtain $\phi = -\pi/2$. For applied frequencies $\omega < \omega_s$ the phase shift increases toward $\phi = 0$, whereas for frequencies $\omega \gg \omega_s$ the phase shift approaches $\phi = -\pi$. Thus moving away from the surface resonance has an influence on the sign reversal in $\chi^{(3)}$ similar to that of absorption in the host medium.

What is the cause of this phase shift between the macroscopic applied field and the field inside an inclusion? Remember that the transmitted electric field for light incident upon an imperfectly conducting surface undergoes a phase shift that depends on its polarization, the conductivity of the surface, and the absorption in the surrounding dielectric (host) medium. We denote this phase shift by ϕ_s for s-polarized light and ϕ_p for p-polarized light. Hence the average phase shift at the surface is $(\phi_s + \phi_p)/2$. At the surface plasmon resonance, however, some of the p-polarized light goes into surface plasmons, whereas s-polarized light does not generate surface plasmons. The average phase shift at the surface is then $(\phi_s + \phi_p - \Delta\phi_p)/2$. Hence the generation of surface plasmons causes a $\Delta\phi_p/2$ change in the average phase shift of the transmitted light. Therefore the phase shift between **e** and **E** is partly determined by the selective coupling of p-polarized photons into plasmons at the surface and partly by the refraction at the interface. Absorption in the host affects the phase shift at a conducting surface because the propagation constant in the host is then complex. Hence moving off resonance and increasing the host absorption both affect the phase shift between **e** and **E**. Note that for a perfect conductor the same phase shift would not occur, however. Thus to the extent that particle size and connectivity (percolation) determine the conductivity (and geometry) of the surface, these factors also determine the phase shift between **e** and **E**.

Although the assumption that $\epsilon \approx \epsilon_h$, which makes Eq. (7) linear in f, allows us to deduce the sign reversal in $\chi^{(3)}$, in practice we have found that one must take into account the full nonlinear relationship between $\chi^{(3)}$ and f to predict correctly the full complex cubic susceptibility at ordinary fill fractions. For example, the real part of $\chi^{(3)}$ may not be linear in f, even for the small fill fractions considered in this study. Moreover, although Eq. (7) predicts only one fill fraction at which $\chi^{(3)}$ changes sign, by necessity there will actually be two fill fractions at which $\chi^{(3)}$ changes sign if $\chi_h^{(3)}$ and $\chi_i^{(3)}$ have the same sign. Equation (3) predicts both of these sign reversals in $\chi^{(3)}$. Hence the usefulness of Eq. (7) is restricted to small fill fractions. Our purpose in introducing it here is simply to allow for a more intuitive understanding of the sign reversal in $\chi^{(3)}$.

At this point one could wonder whether the cancellation that occurs for the imaginary part of $\chi^{(3)}$ might not also occur for the real part. In fact, a cancellation in the real part of $\chi^{(3)}$ can also occur, provided that Re $\chi_h^{(3)}$ and Re $\chi_i^{(3)}$ have the same sign. However, the cancellations in Im $\chi^{(3)}$ and Re $\chi^{(3)}$ are not likely to occur at the same fill fraction. Moreover, if the host material is chosen such that it possesses an electronic negative lensing effect (so that Re $\chi_h^{(3)} < 0$), the real part of $\chi^{(3)}$ will not undergo the same sign reversal and can actually be enhanced. In fact, this possibility is precisely what makes this approach compelling. In this study, however, we limit our discussion to the imaginary part of $\chi^{(3)}$. Experimentally, it will be much easier to demonstrate the cancellation in the imaginary part of $\chi^{(3)}$ than a change in the real part, because the nonlinearity in small metal particles arises primarily from absorptive mechanisms.[3]

2. EXPERIMENTAL PROCEDURE

A. Gold Colloid Preparation

There are many different methods for synthesizing metal colloids.[8] No single method is suited for all applications. The hydrosol route consists of reducing an acid of the metal to produce an aqueous dispersion. Chemical purity can be carefully controlled, and the suspension can be kept quite monodisperse. The recipe of Turkevich *et al.* was followed for this study.[9] A 95-mL solution of $HAuCl_4$ in water containing 5 mg of Au was prepared. The chloroauric acid was then heated to the boiling point, and 5 mL of a 1% solution of sodium citrate in water was added instantaneously under vigorous stirring. The solution quickly turned a pale blue, darkening to a deep red after ~5 min. Decreasing the temperature slows the reaction. The resulting dispersion of Au is kept stable by the repulsion of Cl^- ions surrounding the Au particles. Dialysis can be used to remove excess ions and salt from the solution. A chloride probe, a silver nitrate solution, or a spectrofluorometer can be used to find the chloride content of the dispersion before and after dialysis.[10]

B. Z Scan

The Z scan[11] is a simple, sensitive technique that relies on nonlinear phase shifts to obtain the complex third-order susceptibility. It is essentially a derivative of the ubiquitous single-beam power-in versus power-out transmission measurement[12] but attains greater efficiency by fo-

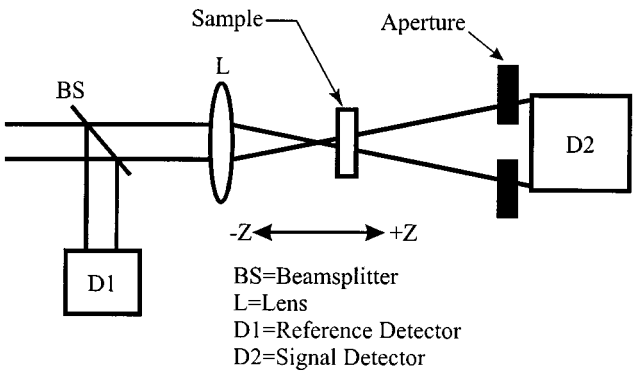

Fig. 1. Z-scan experimental arrangement.[10]

cusing the beam and translating the sample. The technique involves the measurement of the transmittance through an aperture placed in the far field as the sample is translated through the focus of a Gaussian beam, as shown in Fig. 1. In general this technique can be used to measure either refractive or absorptive nonlinearities.

If the aperture is fully opened so the detector collects all the light, then the Z scan detects intensity-dependent absorption. At the focus the irradiance is greatest and thus will produce the greatest effect. If $\mathrm{Im}\,\chi^{(3)} > 0$, then the Z scan will result in a valley, indicative of induced absorption (due to multiphoton absorption or reverse saturable absorption, for instance). If $\mathrm{Im}\,\chi^{(3)} < 0$, then the Z scan will produce a peak, indicating induced transparency (due to saturable absorption, for example). Because the flux from the sample is collected at the detector, the transmitted power can be calculated without having to perform the free-space Fresnel propagation to the aperture. The normalized transmittance can then be expressed as[11]

$$T(z) = \sum_{m=0}^{\infty} \frac{\left(\dfrac{-\beta I_0 L_{\mathrm{eff}}}{1 + z^2/z_0^2}\right)^m}{(m+1)^{3/2}}, \tag{12}$$

where β is the nonlinear absorption coefficient, I_0 is the on-axis peak intensity at the focus, L_{eff} is the effective interaction length, and z_0 is the Rayleigh diffraction length. Typically, if the series converges, only the first few terms are needed for numerical evaluation. Hence the coefficient β can be determined from a fit of this expression to the empirical data.

In this study, to obtain the absorptive nonlinearity we performed open-aperture Z-scan measurements on a gold colloid prepared by the recipe of Turkevich *et al.*[9] and diluted to obtain various concentrations. A frequency-doubled Nd:YAG laser at 532 nm provided 30-ps mode-locked pulses at a repetition rate of 10 Hz. Each dilution was placed in a 1-cm-square quartz cuvette on a track near the focus of the beam. The focal length of the lens was 33 cm, and the FWHM beam diameter was 2.5 mm. The beam waist was measured to be $w_0 = 70\ \mu$m, corresponding to a Rayleigh diffraction length of $z_0 = 2.9$ cm.

3. RESULTS

The results presented here are divided into two sections. In the first section we present the results of open-aperture Z scans of gold in water. The goal is to deduce a value for $\mathrm{Im}\,\chi_i^{(3)}$ by comparing the generalized Maxwell Garnett results with the experimental data. In the second section Z scans of gold colloid in a laser dye solution are presented. In this case our intention is to prove that the nonlinear absorption changes sign for a certain concentration, as predicted by the model.

A. Open-Aperture Z Scans of Gold Colloid

Open-aperture Z scans of various concentrations of gold in water are described here. For each sample the incident peak power was $P_i = 0.51$ MW, corresponding to $I_0 = 5.9$ GW/cm^2. To obtain L_{eff}, we measured the absorbance between 190 and 820 nm, using a UV–visible spectrophotometer. The surface plasmon resonance was clearly visible at 522 nm. The absorbance was measured to be 0.91 for the gold colloid stock solution at 532 nm, which corresponds to an absorption coefficient of $\alpha_0 = 2.1\ \mathrm{cm}^{-1}$ and an effective interaction length of $L_{\mathrm{eff}} = 0.42$ cm. The quartz cuvette and water were used as a baseline scan and were subtracted out of the spectrum. When the colloid was fractionally diluted, the absorbance decreased by the same factor. The refractive index was assumed to be approximately the same as that of water so that $n_0 = 1.33$.

The absorption spectrum is also useful for obtaining the concentration of the gold colloid stock solution. To obtain the volume fill fraction one can use the relation

$$\alpha_0 = \frac{\omega}{n_0 c}\,\epsilon'' = \frac{\omega}{n_0 c}\, f |q_i^2| \epsilon_i''. \tag{13}$$

The imaginary part of ϵ_i can be assumed to be $\epsilon_i'' = 2.4$ from the bulk value. The local field factor is then $q_i = -2.21i$. The absorbance was 0.99 at 522 nm so that $\alpha_0 = 2.3\ \mathrm{cm}^{-1}$ at the peak of the surface plasmon resonance. Solving Eq. (13) for f then yields a volume fraction of 2.2×10^{-6}.

Figure 2 illustrates the experimental data. Error bars represent the standard deviation of 10 averages. We have chosen to plot a subset of the experimental data and to include error bars only in the first curve for clarity. Equation (12) was used to fit a curve to each set of data by varying the adjustable parameter β. Note that, as the focus is approached, the transmittance increases in each case, demonstrating that the colloid is a saturable absorber. Examining more closely the data for the stock solution displayed in Fig. 2 reveals that $|\beta I_0 L_{\mathrm{eff}}| > 1$, making the series diverge in Eq. (12). Therefore the value found for β in this case is not really accurate but is provided only for the purpose of comparison. When the colloid is diluted to 50%, however, the series again converges, and the values presented for β are valid. Note that as the concentration of gold decreases, so does the peak-to-valley transmittance.

The weak nonlinearity of water at 532 nm makes it difficult to ascertain whether the nonlinear absorption in

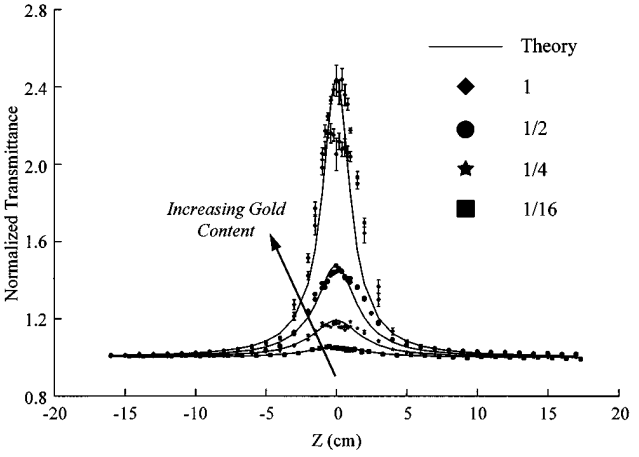

Fig. 2. Open-aperture Z scans at 532 nm and $P_i = 0.46$ MW for a gold colloid stock solution and for solutions fractionally diluted by 1/2, 1/4, and 1/16 from the stock.

Table 1. Change in Nonlinear Absorption with Concentration

Concentration	β (m/W)	Im $\chi^{(3)}$ (esu)	Error (esu $\times 10^{-13}$)
1	-4.5×10^{-12}	-6.4×10^{-12}	± 0.8
1/2	-2.0×10^{-12}	-2.9×10^{-12}	± 1.0
1/4	-9.0×10^{-13}	-1.3×10^{-12}	± 0.8
1/4	-9.1×10^{-13}	-1.3×10^{-12}	± 0.8
1/8	-6.6×10^{-13}	-9.4×10^{-13}	± 0.6
1/16	-2.6×10^{-13}	-3.8×10^{-13}	± 0.4
1/32	-1.5×10^{-13}	-2.1×10^{-13}	± 0.4
1/64	-1.3×10^{-14}	-1.8×10^{-13}	± 0.4

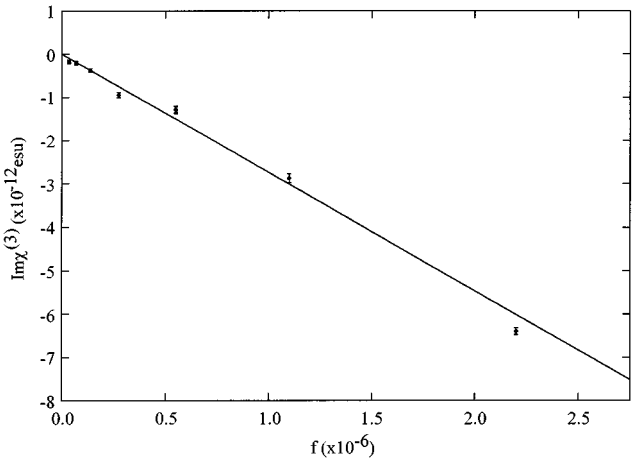

Fig. 3. Nonlinear absorption of the gold colloid. The solid curve is a fit from the Maxwell Garnett theory, where Im $\chi_i^{(3)}$ is a fitting parameter.

fact switches sign. This is not unexpected because, owing to the negligible linear absorption of water at 266 nm, the two-photon transition probability will not be resonantly enhanced. One can, however, use this system to deduce a value for Im $\chi_i^{(3)}$.

Table 1 and Fig. 3 illustrate the change in Im $\chi^{(3)}$ with fill fraction. The relationship between the adjustable parameter β and the imaginary part of the cubic susceptibility is[13]

$$\text{Im } \chi^{(3)} = \frac{\lambda c n_0^2 \beta}{640 \pi^3}, \tag{14}$$

where the quantity on the right-hand side of Eq. (14) must be in Gaussian units and the quantity on the left-hand side is in electrostatic units. Note that the error does not decrease as rapidly as the signal. By treating Im $\chi_i^{(3)}$ as an adjustable parameter, one can fit Eq. (3) or Eq. (7) to the experimental data. The best fit was obtained from Im $\chi_i^{(3)} = (1.1 \pm 0.1) \times 10^{-7}$ esu. This value compares well with the value Im $\chi_i^{(3)} = 5 \times 10^{-8}$ esu found by Bloemer *et al.*[14] and Hache *et al.*[3] and agrees particularly well with the value of 1.1×10^{-7} esu theoretically deduced by Hache *et al.*[3] for the Fermi smearing, or hot-electron, mechanism, which involves transient conduction electron heating. This comparison should not be taken too seriously, however, because the refractive index of the metal may not change linearly with the temperature of the conduction electrons for the intensities used here.

The average diameter of the gold particles produced by the recipe used in this study is ~20 nm. Bloemer *et al.*[14] found that, for particle diameters below ~15 nm, lattice heating did not contribute significantly to the nonlinearity for laser pulses of the same duration as used here. For larger particles lattice heating contributed only weakly, resulting in a slight size dependency in $\chi^{(3)}$. Hence, in addition to the possibility of saturation of the hot-electron contribution, a slight contribution from lattice heating could also be present.

B. Open-Aperture Z Scans of Gold Colloid in HITCI

To show conclusively the sign reversal caused by the surface plasmon modification of the local field factor, we need to examine a more complex system. Materials were sought for the host that would have a strong absorptive nonlinearity so the sign reversal could easily be resolved. Unfortunately, assimilation of metal particles into highly nonlinear solid state materials is difficult through traditional chemical techniques. Ion implantation is an excellent alternative but is not readily available in most laboratories. To bypass these difficulties we decided not to pursue solid-state assimilation but rather to use a liquid host. The search for the combination of aromaticity (for high nonlinearity), water solubility (for colloid compatibility), and the correct wavelength dependence (strong linear absorption at 266 nm to maximize the two-photon transition probability at 532 nm) proved a difficult task. Pyradine, acetone, 8-quinolinol, paranitroaniline, and other aromatic, water-soluble liquids were analyzed. Although a flourescence study by Giordamaine and Howe[12] indicated that the onset of two-photon absorption should occur in these liquids at an irradiance just lower than required for Raman scattering, direct TPA measurements are generally less sensitive. Raman scattering and self-focusing generally masked any TPA that might have been present.

Laser dyes such as *p*-terphenyl that have strong linear absorption at 266 nm should provide strong TPA at 532 nm, but water-soluble derivatives are not readily available. This is true in general for dyes with strong absorption in the blue part of the spectrum. Finally a material was found that had strong positive nonlinear absorption and low nonlinear refraction and was water soluble and semicompatible with the colloid. Instead of TPA, however, the nonlinear mechanism was reverse saturable absorption. The system consisted of a known reverse saturable absorber, 1, 1′, 3, 3, 3′, 3′-hexamethylindotricarbocyanine iodine (HITCI), in methanol and water. The proportions of dye, methanol, and water were held fixed. Because these chemicals form a solution they can be considered a single component, although their chemical association should be accounted for by a modification of the local field factor as described by Fröhlich.[15] The other component was gold. A colloid of gold in HITCI is stable only for a short time, so the measurements had to be taken quickly.

The proportions of the various components are illustrated in Table 2. Note that the same amount of dye, methanol, and water is used in each case and that the

Table 2. Component Proportions for HITCI–Au Composite

Curve Number[a]	Gold Colloid (mL)	Water (mL)	123-μM HITCI (mL)	Methanol (mL)
1	0	2.75	0.4	0.6
2	0.5	2.25	0.4	0.6
3	1.0	1.75	0.4	0.6
4	1.5	1.25	0.4	0.6
5	1.9	0.85	0.4	0.6
6	2.0	0.75	0.4	0.6
7	2.2	0.55	0.4	0.6
8	2.5	0.25	0.4	0.6
9	2.75	0	0.4	0.6

[a] Fig. 4.

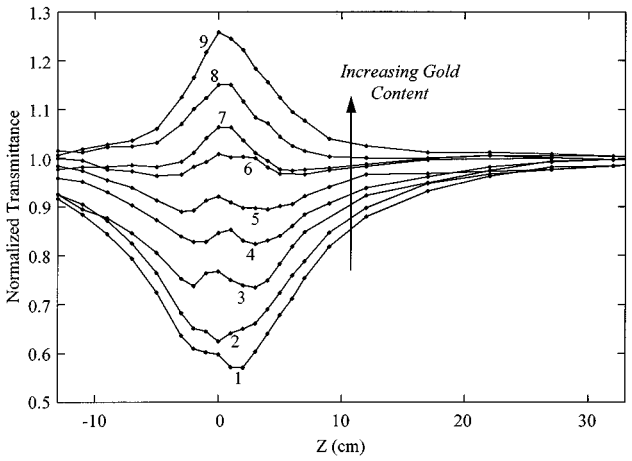

Fig. 4. Nonlinear absorption of various concentrations of gold in HITCI. The nonlinear absorption is canceled near curve 6.

only variable is the concentration of gold. The Z scans for various concentrations of gold are displayed in Fig. 4. For each Z scan the peak power was $P_i = 0.16$ MW and the on-axis peak irradiance at focus was $I_0 = 2.1$ GW/cm^2. It can clearly be seen that the nonlinear absorption changes sign near curve 6. The experiment was repeated several times, and the sign reversal was obvious each time.

Note that curves 1–5 display a valley, which is indicative of reverse saturable absorption. At the focus, however, a small secondary peak is observed. This peak corresponds to a saturation of the nonlinear absorption and was first reported by Swatton *et al.*[16] A four-level semiclassical model was used to describe the absorption of the dye.

4. SUMMARY AND CONCLUSIONS

This investigation has demonstrated a method for eliminating unwanted nonlinear absorption, such as two-photon absorption and reverse saturable absorption, through a materials architecture approach. There are two different metal volume fractions at which the imaginary part of $\chi^{(3)}$ vanishes. Previous studies that ignored the nonlinearity of the host failed to predict the more useful lower concentration at which Im $\chi^{(3)} = 0$. The sign change in $\chi^{(3)}$ was shown to be a result of a modification of the local field factor at the surface plasmon resonance. The local field factor becomes mainly imaginary as a result of a phase shift between the applied field and the field inside an inclusion. Using the Z-scan technique, we demonstrated conclusively the sign reversal in Im $\chi^{(3)}$ by using a host with a strong absorptive nonlinearity. It is hoped that in the future, through techniques such as ion implantation or through functionalization of the gold particles, metal colloids will be readily produced in highly nonlinear solid-state materials such as conjugated polymers.

We deduced the nonlinearity of the metal particles by comparing the nonlinear susceptibilities of the colloid, measured with the Z-scan technique, with the predictions of the Maxwell Garnett model. The experimental values were fitted to the theory for several different metal concentrations. A value of Im $\chi_i^{(3)} = 1.1 \times 10^{-7}$ esu was obtained, which corresponds closely to the theoretical value for the Fermi smearing mechanism presented by Hache *et al.*[3]

Because the nonlinearity of the metal cannot be measured directly, the generalized Maxwell Garnett model cannot be tested for its validity by use of these systems. One area of ambiguity is the applicability of the local field factor. In pure nonpolar host materials the Lorentz local field factor is appropriate. However, for polar or mixed solvents, for example, the local field factor may have to be modified to take into account molecular polarity[17] or chemical association.[15] It is not known how dramatically this constraint might change the Maxwell Garnett results. It would be useful, therefore, to be able to measure the inherent nonlinearity of the metal directly.

Throughout this discussion we have assumed that the linear dielectric constant of the metal can be approximated by the bulk value. In future publications we shall discuss the particle size dependence of the effective $\chi^{(3)}$ and its relationship to the size dependency of the local field factors. Further, we shall examine the real part of the cubic susceptibility and present a simple method for determining whether candidate materials can be improved by use of a composite geometry.

ACKNOWLEDGMENTS

The authors gratefully acknowledge discussions with A. T. Rosenberger, M. J. Bloemer, and C. M. Bowden on the contents of this work and the invaluable assistance of R. J. Gehr, M. S. Paley, D. O. Frazier, and J. S. Johnson. The research of D. D. Smith was supported by the Center Director's Discretionary Fund at Marshall Space Flight Center. The research of G. Fischer was supported by the U.S. Air Force Palace Knight Program.

REFERENCES

1. V. K. Mizrahi, K. W. Delong, G. I. Stegeman, M. A. Saifi, and M. J. Andrejco, "Two-photon absorption as a limitation to all-optical switching," Opt. Lett. **14**, 1140 (1989).
2. K. W. Delong and G. I. Stegeman, "Two-photon absorption as a limitation to all-optical waveguide switching in semiconductors," Appl. Phys. Lett. **57**, 2063 (1990).
3. F. Hache, D. Ricard, C. Flytzanis, and U. Kreibig, "The op-

tical Kerr effect in small metal particles and metal colloids: the case of gold," Appl. Phys. A **47**, 347 (1988).
4. J. C. Maxwell Garnett, "Colours in metal glasses and in metallic films," Philos. Trans. R. Soc. London **203**, 385 (1904); **205**, 237 (1906).
5. D. Ricard, P. Rousignol, and C. Flytzanis, "Surface-mediated enhancement of optical phase conjugation in metal colloids," Opt. Lett. **10**, 511 (1985).
6. J. W. Sipe and R. W. Boyd, "Nonlinear susceptibility of composite optical materials in the Maxwell Garnet model," Phys. Rev. A **46**, 1614 (1992).
7. D. A. G. Bruggeman, "Calculation of various physical constants of heterogeneous substances. Part I. Dielectric constant and conductivity of mixtures of isotropic substances," Ann. Phys. (Leipzig) **24**, 636 (1935).
8. J. A. A. J. Perenboom, P. Wyder, and F. Meier, "Electronic properties of small metallic particles," Phys. Rep. **78**, 173 (1981).
9. J. Turkevich, P. C. Stevenson, and J. Hillier, "A study of the nucleation and growth processes in the synthesis of colloidal gold," Discuss. Faraday Soc. **11**, 55 (1951).
10. L. Sibille, "Study by gravimetry, fluorometry, and calorimetry of crystallizing tetragonal lysozyme solutions," Ph.D. dissertation (Institut National des Sciences Appliquées des Toulouse, Toulouse, France, 1994).
11. M. Sheik-Bahae, A. A. Said, T. Wei, D. J. Hagan, and E. W. Van Stryland, "Sensitive measurement of optical nonlinearities using a single beam," IEEE J. Quantum Electron. **26**, 760 (1990).
12. J. A. Giordmaine and J. A. Howe, "Intensity-induced optical absorption cross section in CS_2," Phys. Rev. Lett. **11**, 207 (1963).
13. Y. M. Cheung and S. K. Gayen, "Optical nonlinearities of tea studied by Z-scan and four-wave mixing techniques," J. Opt. Soc. Am. B **11**, 636 (1994).
14. M. J. Bloemer, J. W. Haus, and P. R. Ashley, "Degenerate four-wave mixing in colloidal gold as a function of particle size," J. Opt. Soc. Am. B **7**, 790 (1990).
15. H. Fröhlich, *Theory of Dielectrics* (Oxford U. Press, London, 1958).
16. S. N. R. Swatton, K. R. Welford, S. J. Till, and J. R. Sambles, "Nonlinear absorption of a carbocyanine dye 1, 1′, 3, 3, 3′, 3′-hexamethylindotricarbocyanine iodide using a Z-scan technique," Appl. Phys. Lett. **66**, 1868 (1995).
17. L. Onsager, "Electric moments of molecules in liquids," J. Am. Chem. Soc. **58**, 1486 (1936).